

PAPER • OPEN ACCESS

Combatting rain erosion of offshore wind turbine blades by co-bonded thermoplastic-thermoset hybrid composites

To cite this article: Jamal Seyyed Monfared Zanjani *et al* 2020 *IOP Conf. Ser.: Mater. Sci. Eng.* **942** 012024

View the [article online](#) for updates and enhancements.

239th ECS Meeting

with the 18th International Meeting on Chemical Sensors (IMCS)

ABSTRACT DEADLINE: DECEMBER 4, 2020



May 30-June 3, 2021

SUBMIT NOW →

Combatting rain erosion of offshore wind turbine blades by co-bonded thermoplastic-thermoset hybrid composites

Jamal Seyyed Monfared Zanjani*, Ismet Baran and Remko Akkerman

Faculty of Engineering Technology, University of Twente, 7500AE Enschede, The Netherlands

*j.seyyedmonfaredzanjani@utwente.nl

Abstract. An integrated thermoplastic-thermoset hybrid leading edge protection system is developed based on the co-bonding process. Co-bonding is a joining method in which a pre-fabricated part joints with a thermoset composite during the curing process. In such a multi-material hybrid design, the reliability of the bonding between the prefabricated protection layer and the main body of the blade is of crucial importance to prevent any delamination failures. Nevertheless, the adhesion of prefabricated thermoplastics to the thermoset remains a challenge as the interphase between two dissimilar materials is prone to form defects and irregularities. Such interface defects may lead to early failure and reduced structural integrity of the components. Therefore, the focus of this study is on achieving a strong, and reliable bonding between the prefabricated thermoplastic leading edge protection system and thermoset main body of the blade. In this study, the effect of processing temperature on the interphase quality and thickness during the co-bonding process is investigated. Next, mechanical characteristics and microstructure of the interphases are examined by Vickers' microhardness tests. The effect of processing condition on the fracture toughness of structure is examined by climbing drum peel tests (CDP). Finally, fractography investigations are used to provide an understanding of failure mechanisms and its correlations with interphase morphology and microstructure.

1. Introduction

The latest manufactured wind turbine blades have reached a length of over a hundred meters where the tip speed can be higher than 100 m/s. The high tip speed of blades and extremely harsh environment of offshore sites present a new challenge in terms of leading-edge erosion by the impact of objects such as raindrops. Rain erosion damages at the leading-edge of wind blades significantly reduce the aerodynamic efficiency and consequently jeopardize the overall integrity of the blades and also decrease the energy production efficiency. The reduction in energy production imperils the price competitiveness of the wind-energy to non-sustainable energy sources. Therefore, a more reliable and durable protection layer that overcomes the rain erosion in wind blades is urgently needed to increase the uptime and productivity of off-shore wind farms and eliminate the costly blade repairs.

Engineering thermoplastics have shown to be more damage tolerant than their thermoset counterparts in many applications for the harsh environment [1]. Therefore, the main objective of this study is to integrate a thermoplastic protection layer as a durable leading edge protection system in the leading edge of the wind turbine blades as schematically presented in Figure 1. Nevertheless, the joining of the thermoplastics leading edge protection to the thermoset of the main body of the blade is a challenging task due to their chemical, physical and mechanical dissimilarities. In such a multi-material hybrid



design, the reliability of the bonding between the protection layer and the main body of the blade is of crucial importance to prevent any delamination failures as shown in Figure 1. Such defected interphase may lead to early failure and reduced structural integrity of the components. Therefore, the focus of this study is on achieving a strong, defect-free, and reliable joining between thermoset and thermoplastic materials.

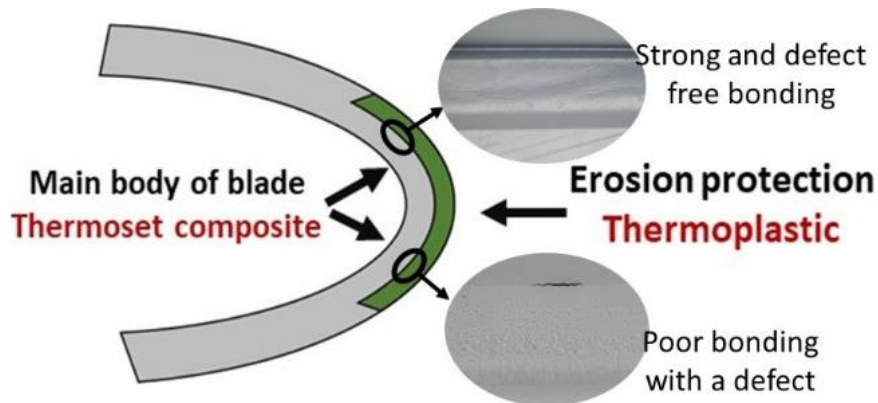


Figure 1. Integrated leading-edge protection by thermoplastic with defected and defect-free bonding.

Various methods have been developed for the joining of polymeric composites including mechanical fastening, welding, adhesive bonding, co-curing, and hybrid joints. Nevertheless, all these joining methods have disadvantages in terms of being unreliable, labor-intensive, time-consuming and, expensive [2]. An alternative and effective joining method for composites is co-bonding where an uncured part joins with one or more cured parts through a single step process [3, 4]. The co-bonding method can be applied for jointing both similar or dissimilar materials including thermoplastics to thermosets. Co-bonding eliminates the needs for mechanical fasteners, and adhesives resulting in a more effective joining for many applications.

It is known that the interface between two parts in the co-bonding process is controlled by their thermodynamic affinity and physical interactions in between and also the curing process of the reactive resin [5]. Nonetheless, the complete understanding of the interdiffusion of a reactive resin into the thermoplastic structure during the co-bonding process remains largely uncovered due to the several challenges and complexities concerning the changes in the properties of the thermoset resin, and unclear diffusion mechanisms.

In this study, the effect of processing temperature on the interphase quality formed between acrylonitrile butadiene styrene (ABS) as the thermoplastic leading edge protection system and unsaturated polyester resin (UPR) as the thermoset during the co-bonding process is investigated. Initially, the effect of three different manufacturing temperatures of 25 °C, 35 °C and 50°C on the interphase thickness are studied. Interphase formation mechanisms are identified and correlated to interphase thickness through the curing kinetics, and rheological changes of the resin. Next, mechanical characteristics and microstructure of the interphases are examined by Vickers' microhardness tests. The effect of processing condition on the bonding quality and the fracture toughness of structure is examined by climbing drum peel tests (CDP). Finally, the fracture surface analyses are performed and insight on various crack propagation mechanisms contributing to bonding quality are recognized.

2. Experimental and Methods

2.1. Materials

An industrial medium reactive orthophthalic unsaturated polyester resin (UPR) system designed for resin transfer molding and vacuum assisted resin transfer molding processes was used as the thermoset resin. A room temperature activated liquid peroxide system specialized for the unsaturated polyester

with long working time (gel time) was used as an initiator. A glass fabric with a 750 g/m² unidirectional roving reinforced (660 g/m²) with random filament and stitching (90 g/m²) on the back was used as the reinforcement. Acrylonitrile butadiene styrene (ABS) in the sheet form was used as thermoplastic material in this study with the grade name of VIKUREEN ABS PLAAT GLANS WIT 0291 known to have a strong resistance to corrosive chemicals and/or physical impacts.

2.2. Composite manufacturing and sample preparation

The effect of processing temperature on the interphase thickness was studied by vertically placing ABS specimens with dimensions 15 mm × 15 mm × 3 mm in the middle of a cylindrical embedding mold with a diameter of 25 mm by using a couple of metallic clamping rings. Next, degassed UPR resin mixture was poured onto the ABS specimens until the resin completely covered the specimen. Prepared specimens and molds were immediately placed in a preheated oven fixed at the set temperatures of 25 °C, 35 °C, and 50 °C for 24 hrs followed by a post-curing at 60 °C for 24 hrs.

Next to the infusion of the pure UPR onto the ABS, three different hybrid sandwich composites were manufactured to analyze the effect of process temperature on the fracture toughness by employing a Climbing Drum Peel (CDP) test. Figure 2 represents the stacking sequence of the composites where initially a layer of UD glass fabric was placed on the mold surface followed by placing an ABS sheet with a thickness of 3 mm and another fabric layer on top. Then the stack was impregnated with degassed UPR through vacuum-assisted resin transfer molding. The curing was performed at three different temperatures of 25 °C, 35 °C, and 50 °C for 24 hrs followed by a post-curing at 60 °C for 24 hrs.

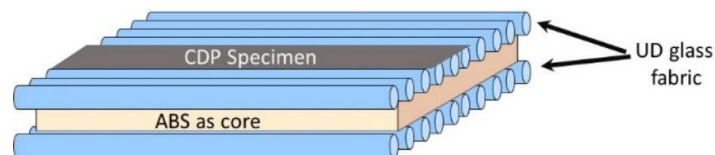


Figure 2. Schematic representation of stacking of hybrid sandwich composite plates.

2.3. Characterizations

The polished cross-section of interphases formed between the co-bonded ABS and UPR systems at various processing conditions were analyzed by using a Keyence VHX-5000 digital microscope equipped with a VH-100UR lens. The interphase thicknesses were measured for each temperature at mid-section of interface far from the clamps and obtained from at least three specimens.

The viscosity and gel time of the UPR were measured using the Anton Paar-Physica MCR 501 rheometer in “plate–plate” mode. All the measurements were performed by using circular aluminum plates of 25 mm diameter in oscillatory mode at a 0.5% strain and a 1 Hz with a plate-plate spacing of 0.3 mm. The viscosity of resin at different temperatures were measured for UPR resin without mixing with the initiator to eliminate the cure effect on viscosity. The temperature-dependent gel time of the resin, as an indication of the cure kinetics of UPR resin, was estimated from the crossing point of storage modulus (G') and loss modulus (G'') of UPR mixture including the liquid peroxide [6].

The Vickers microhardness test was used to probe the mechanical response at the UPR-ABS interphase. Vickers microhardness mapping was conducted using the LECO LM100AT micro-hardness tester by applying a load of 10 gr and an indent spacing of 100 μm . The Vickers diamond pyramid hardness number, HV, was defined as the ratio of the applied load, P, to the pyramidal contact area of the indentation, $H_v = \alpha P/d^2$, where d was the diagonal length of the resultant impression, and α was defined as 1.8544 for Vickers indenter [7].

Climbing Drum Peel (CDP) test based on ASTM Standard D1781 was employed to evaluate the quality of bonded joints between the UPR skin (laminates) and ABS core in the sandwich hybrid composites. The test was performed using a 1 kN load cell at a displacement rate of 25 mm/min. The specimens were cut as 300 mm in length, 10 mm in width as shown in Figure 2. In this test, the critical strain energy release rates were calculated by using Eq 1 as:

$$G_c = \frac{F_d - F_w}{w} \frac{r_2 - r_1}{r_1} \quad (1)$$

where F_w was the force required to overcome the drum weight and to wind the peel arm around the drum, F_d was the force contribution related to the propagation of debonding, w was the width of the specimen and r_1 and r_2 were the radii of the drum and the flanges as 100 mm and 130 mm, respectively. Further details of CDP can be found in [8]. Afterward, fracture analyses of the fracture surfaces after the CDP test were performed using a Keyence VHX-5000 digital microscope.

3. Results and discussion

3.1. Effect of processing temperature on the interphase

Figure 3a reveals the morphology of ABS-UPR interphases fabricated at 25 °C and Figure 3b exhibits the average interphase thickness formed at different temperatures of 25 °C, 35 °C and 50 °C. It is seen that thickness of ABS-UPR interphase prepared at 25 °C was about 710±20 μm while an increase in temperature to 35 °C decreased the interphase thickness to 635±10 μm. This reduction in the interphase thickness by an increase in the temperature from 25 °C to 35 °C was correlated with the acceleration in the cure kinetics of the resin and consequently limited time available for diffusion and interphase formation before solidification of the thermoset resin. To elaborate it is seen in Table 1 that by an increase in temperature from 25 °C to 35 °C, the gel time of the UPR considerably decreased from 12600 S to 3960 S associated with 8640 S shorter gel time. It is worth noting that gel time is an indication of cure kinetics of the resin and it defines the time in which resin switches from a viscous liquid to a semi-solid gel. Herein, gel time was assumed as the time where the diffusion process stopped. Therefore, such a reduction in gel time restricted the diffusion time and resulted in a shorter interphase region. On the other hand, the increase in temperature let to a drop in viscosity of the resin from 1.51 Pa.S at 25 °C to 0.78 Pa.S at 35 °C which favors the increase in the interphase thickness. However, the observed decrease in the interphase thickness showed that the reduction of gel time is more effective than the reduction of resin viscosity on interphase thickness by increasing the temperature from 25 °C to 35 °C. Nonetheless, a further increase in temperature from 35 °C to 50 °C resulted in an increase of interphase thickness to 665±10 μm. This increase in the interphase is associated with the significant reduction of resin viscosity at elevated temperature which reached to 0.35 Pa.S which enhanced the diffusion process and increased the interphase thickness while gelation time only decreased by 3120 S. Thus, the extent of changes in both viscosity and also gelation time are determinant factors of the interphase thickness.

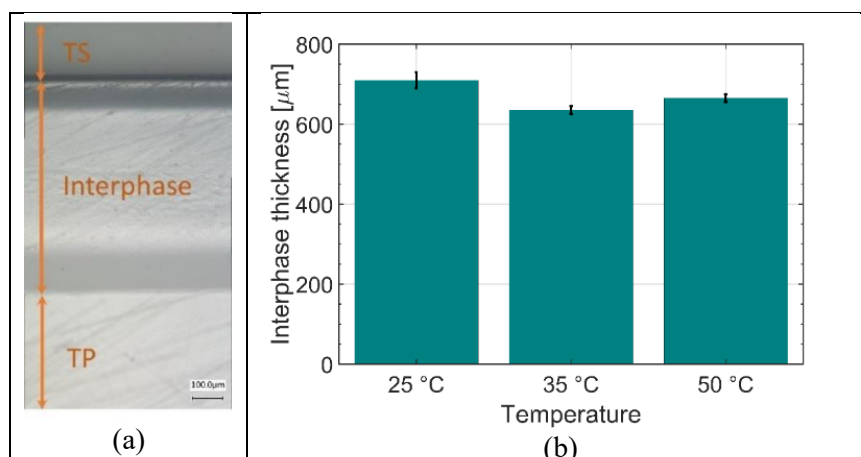


Figure 3. Microscopic view of ABS-UPR interphase fabricated at 25 °C and thickness variation by temperature.

Table 1. Gel time and viscosity of UPR at different temperature.

	25 °C	35 °C	50 °C
Gel time (S)	12600	3960	840
Viscosity (Pa.S)	1.51	0.78	0.35

3.2. Interphases mechanical response by microhardness

Figure 4a shows the variations of Vickers microhardness in the vicinity of the interphase prepared at 25 °C. It was observed that the hardness at the interphase was lower than both cured UPR and ABS. The softer interphase uncovered the plasticizer effect of unreacted UPR diffused into ABS. It also revealed that a significant amount of diffused resin into ABS remained unreacted due to the limited access to reaction components at the interphase area. Figure 4b discloses the average Vickers hardness value at interphase region for specimens fabricated at different temperatures. It was noticed that the average Vickers hardness value at interphase was correlated with the processes temperature and an increasing temperature resulted in an increase in interphase hardness. To elaborate, the average Vickers hardness at the interphase for specimens fabricated at 25 °C measured to be 6.39 ± 0.90 while the increase of processing temperature to 35 °C and 50 °C resulted in hardness at the interphase of 7.28 ± 0.82 and 7.93 ± 0.94 , respectively. This increasing trend in hardness value at interphase for specimens by increasing the manufacturing temperatures is associated with the concentration of resin at the interphase area which was decreased by an increase in temperature due to the acceleration in resin cure kinetics and diffusion kinetics.

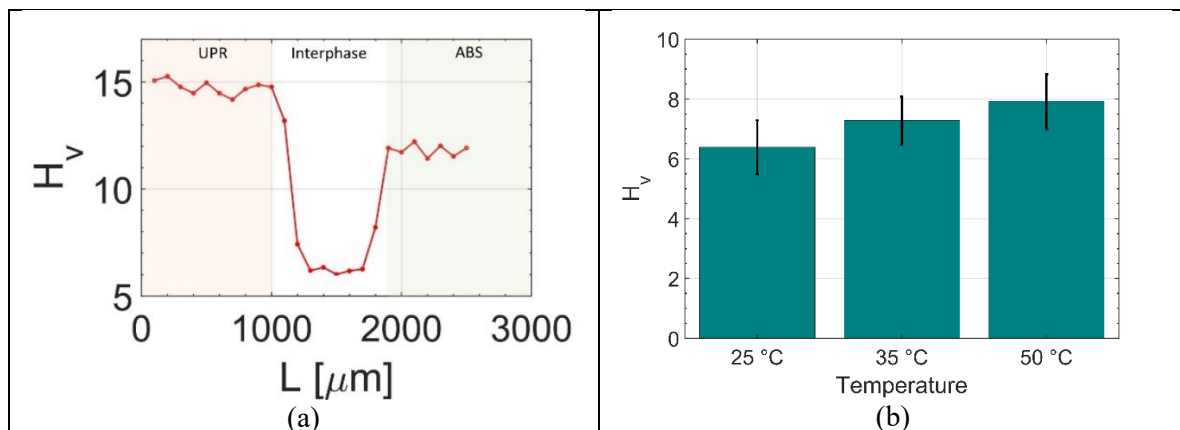


Figure 4. (a) Vickers microhardness for UPR-ABS prepare at 25 °C, and (b) variation of interphase hardness by manufacturing temperature.

3.3. Fracture toughness by climbing drum test

Figure 5a displays the typical CDP test curve obtained for a specimen prepared at 25 °C. The F_w is measured to be 160 N and the average force for crack propagation was measured in the crack propagation area as shown in Figure 5a. Figure 5b exhibits the fracture toughness measured for specimens fabricated at three different temperatures of 25 °C, 35 °C and 50 °C. It was observed that the highest fracture toughness was measured for specimens manufactured at 25 °C as 3.45 ± 0.3 N/mm. However, an increase in manufacturing temperature to 35 °C reduced the fracture toughness to 1.44 ± 0.2 N/mm. A further increase in processing temperature to 50 °C slightly increased the fracture toughness to 1.8 ± 0.2 N/mm.

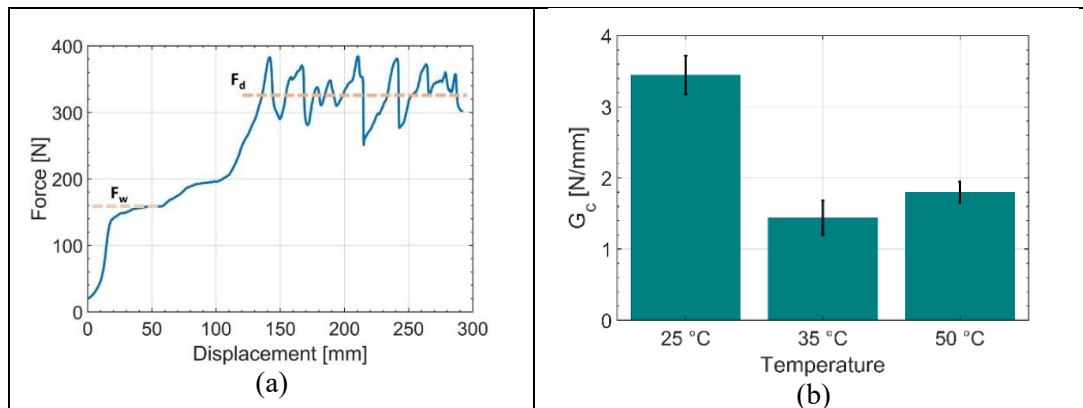


Figure 5. (a) Typical force-displacement curve for CDP of UPR-ABS specimen fabricated at 25 °C, and (b) fracture toughness for specimens prepared at different temperatures.

3.4. Fractography analysis

Figure 6 depicts the fracture surface of glass fabric reinforced thermoset skin after CDP tests. It is seen that two different mechanisms were contributing to crack propagations namely interface failure and cohesive failure. In the interface failure, skin and core were debonded at their interface without any sign of their attachment. On the other hand, in the cohesive failure area residues of ABS were remained on the skin surface. Since the cohesive strength of ABS is much higher than the UPR-ABS interfacial strength, cohesive failure enhanced the fracture toughness measured by CDP tests. Figure 6 reveals that the fracture surface of the specimen manufactured at 25 °C contained a high level of cohesive failure which was complied with its comparative higher fracture toughness as observed in Figure 5b compare to other specimens. Furthermore, it was observed in Figure 3b that the specimen manufactured at 25 °C formed the thickest interphase and therefore higher level of interdiffusions which reflected in higher cohesive failure and consequently higher fracture toughness for these specimens. On the other hand, the fracture surface of specimen manufactured at 35 °C, showed a very low amount of cohesive failure which is also coordinated with its lowest fracture toughness and the thinnest interphase thickness compared to other specimens. Alternatively, specimen prepared at 50 °C, showed a moderate level of cohesive failure compared to other specimens in which the number of cohesive failures was alike to specimen fabricated at 25 °C while their size was much smaller which was in correlation to its intermediate interphase thickness and fracture toughness values.

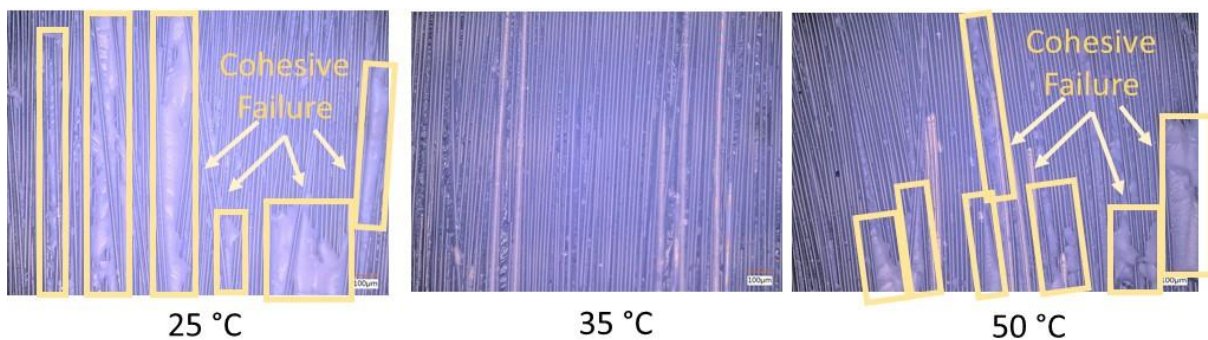


Figure 6. Fracture surface on thermoset skins after CDP test.

4. Conclusions

An integrated leading edge protection system based on co-bonding of an engineering thermoplastics to the thermoset main body of blades is proposed for rain erosion inhibition. In the proposed design, the effect of processing conditions on the bonding quality of ABS as the thermoplastic protection to polyester composite as the main body of the blade were studied during the co-bonding process. The

bonding quality was correlated with the cure kinetics and interphase thickness of the resin. It was observed that the interphase size changed with the processing temperature and it was linked to the thermal changes in the viscosity and cure kinetics of UPR. Microhardness tests showed that the hardness of interphase was lower than both ABS and UPR regions due to the plasticization effect of UPR molecules at the interphase. An increasing trend in hardness value at interphase by increasing the manufacturing temperatures were observed. CDP tests were performed and maximum fracture toughness was obtained for specimens fabricated at 25 °C while specimens manufactured at 35 °C present the minimum fracture toughness. Fracture surface analyses revealed that two different mechanisms were contributing to crack propagations namely interface failure and cohesive failure. Consequently, it was concluded that fracture toughness of specimens was closely related to the level of cohesive failure and specimen with thicker interphase resulted in higher cohesive failure and fracture toughness whereas thinner interphase led to lower cohesive failure and consequently lower fracture toughness.

Acknowledgment

Authors gratefully acknowledge the research program Talent Scheme (Veni) with project number 15897, which is (partly) financed by the Netherlands Organization for Scientific Research (NWO) and TKI-Wind op Zee Topsector Energy subsidy from the Ministry of Economic Affairs, the Netherlands with the reference number TEWZ118008. Authors are also thankful to LM Wind Power for consultations during the project and supply polyester resin.

References

- [1] Seyyed Monfared Zanjani J, Saner Okan B and Menciloglu Y 2016 Manufacturing of multilayer graphene oxide/poly(ethylene terephthalate) nanocomposites with tunable crystallinity, chain orientations and thermal transitions, *Mater. Chem. Phys.* **176**, 58-67
- [2] Karakaya N, Papila M and Özkoç G 2020 Overmolded hybrid composites of polyamide-6 on continuous carbon and glass fiber/epoxy composites: 'An assessment of the interface' *Compos. Part A Appl. Sci. Manuf.* **131**, 105771
- [3] Baran I 2017 Warpage prediction in over-infusion process of glass/polyester composite laminates. *21st International Conference on Composite Materials*, 2017,
- [4] Leone C and Genna S 2018 Effects of surface laser treatment on direct co-bonding strength of CFRP laminates, *Compos. Struct.* **194**, 240-51
- [5] Stavrov D and Bersee H E N 2005 Resistance welding of thermoplastic composites-an overview *Compos. Part A Appl. Sci. Manuf.* **36**, 39-54
- [6] Hsu C and Lee L J 1993 Free-radical crosslinking copolymerization of styrene/unsaturated polyester resins: 3. Kinetics-gelation mechanism *Polymer*, **34**, 4516-23
- [7] Gong J, Wu J and Guan Z 1999 Examination of the indentation size effect in low-load vickers hardness testing of ceramics. *Eur. Ceram.* **19**, 2625-31
- [8] Daghia F and Cluzel C 2015 The Climbing Drum Peel Test: An alternative to the Double Cantilever Beam for the determination of fracture toughness of monolithic laminates *Compos. Part A Appl. Sci. Manuf.* **78**, 70-83